Heliyon 10 (2024) e32482

Contents lists available at ScienceDirect

Heliyon

journal homepage: www.cell.com/heliyon

Research article

Serum metabolomics study reveals a distinct metabolic diagnostic model for renal calculi

Yunhe Xiong [a,1], Qianlin Song [a,1], Shurui Zhao [c], Chuan Wang [a], Hu Ke [a], Wenbiao Liao [a], Lingchao Meng [a], Lingyan Liu [b,**], Chao Song [a,*]

[a] *Department of Urology, Renmin Hospital of Wuhan University, Jiefang Road 238, 430060, Wuhan, Hubei Province, People's Republic of China*
[b] *Beijing Area Major Laboratory of Peptide and Small Molecular Drugs, Engineering Research Center of Endogenous Prophylactic of Ministry of Education of China, School of Pharmaceutical Sciences, Capital Medical University, Beijing, People's Republic of China*
[c] *Core Facilities Center, Capital Medical University, Beijing, People's Republic of China*

ARTICLE INFO

Keywords:
Renal calculi
Metabolomics
UPLC–MS
Glycerophospholipid
Plasmalogen

ABSTRACT

Renal calculi (RC) represent a prevalent disease of the urinary system characterized by a high incidence rate. The traditional clinical diagnosis of RC emphasizes imaging and stone composition analysis. However, the significance of metabolic status in RC diagnosis and prevention remains unclear. This study aimed to investigate serum metabolites in RC patients to identify those associated with RC and to develop a metabolite-based diagnostic model. We employed non-targeted metabolomics utilizing ultra-performance liquid chromatography–mass spectrometry (UPLC–MS) to compare serum metabolites between RC patients and healthy controls. Our findings demonstrated significant disparities in serum metabolites, particularly in fatty acids and glycerophospholipids, between the two groups. Notably, the glycerophospholipid (GP) metabolic pathway in RC patients was significantly disrupted. Logistic regression models using differentially abundant metabolites revealed that elevated levels of 2-butyl-4-methyl phenol and reduced levels of phosphatidylethanolamine (P-16:0/22:6(4Z,7Z,10Z,13Z,16Z,19Z)) had the most substantial effect on RC risk. Overall, our study indicates that RC induces notable alterations in serum metabolites and that the diagnostic model based on these metabolites effectively distinguishes RC. This research offers promising insights and directions for further diagnostic and mechanistic studies on RC.

1. Introduction

As one of the most prevalent urinary system diseases, renal calculi (RC) significantly affect 10–15 % of the global population [1,2] and have been acknowledged as an epidemic on par with obesity and type 2 diabetes [3]. The recurrence rate of calculi is alarmingly high, with a 50 % incidence within 5–10 years following the initial attack [4]. Patients with cystinuria receive an average of 10.6 interventions per patient [5], leading to a substantial economic burden. Additionally, RC can cause severe complications, including urinary tract infections, abdominal pain, hydronephrosis, and renal dysfunction.

* Corresponding author.
** Corresponding author.
E-mail addresses: Lingyan@ccmu.edu.cn (L. Liu), drsongchao@whu.edu.cn (C. Song).
[1] These authors contributed equally to this work and shared the first authorship.

https://doi.org/10.1016/j.heliyon.2024.e32482
Received 12 March 2024; Received in revised form 3 June 2024; Accepted 4 June 2024

Multiple factors contribute to the development of RC [1]. The risk of RC increases with age, typically manifesting between the ages of 30 and 50. Sex is another crucial determinant, as men exhibit a 2–4 times greater risk, incidence, and prevalence of RC than women [6]. This discrepancy can be attributed to the androgen induced increase in calcium oxalate excretion and deposition in the kidneys, which are the primary risk factors for RC formation. Conversely, estrogen reduces uric acid excretion. The composition of the stones is also complex, with 79 % primarily composed of calcium salts (oxalate and phosphate), followed by uric acid stones at 16.5 %, a combination of calcium salts and uric acid at 2 %, other salts at 1.9 %, and cystine at 0.6 % [7].

In recent years, there has been a rapid increase in the use of metabolomics for the treatment of RC due to the development and popularization of metabolomics technology. Some researchers have already conducted metabolic profiling on the urine of RC patients using 1H NMR [8,9] and targeted amino acid methods [10]. Reports on untargeted metabolomics [11], lipid metabolism [12], and bile acid metabolism [13] in animal models of RC are also on the rise. However, there is a relative scarcity of serum-targeted metabolomics, with the focus being primarily on pediatric RC patients [14]. Therefore, there is a need for further exploration of RC serum metabolic profiles, as they may contain potential biomarkers for diagnosis and key molecules relevant to their formation.

To address this need, this study used ultra-performance liquid chromatography–mass spectrometry (UPLC–MS) technology to detect and analyze serum metabolites in both healthy controls (HC) and RC patients. The aim of this study was to provide new evidence of differential serum metabolic profiles in RC patients, identify potential molecular targets for RC diagnosis, and elucidate the mechanisms underlying RC formation.

2. Materials and methods

2.1. Sample collection

Serum samples were collected from 45 patients with RC and 48 HC. The study protocol was approved by the Research Ethics Board of Renmin Hospital of Wuhan University (WDRY2023-K183), adhering to the ethical standards of the institutional and/or national research committee and in accordance with the 1964 Helsinki Declaration and its later amendments or comparable ethical standards. Informed consent was obtained from all participants. The inclusion criteria for RC patients were as follows: 1. The diagnosis of RC was made according to the European Association of Urology guidelines for urolithiasis. 2. Age between 18 and 65 years. 3. Good general health. The exclusion criteria were as follows: 1. Renal and ureteral obstruction or malformation. 2. Severe hydronephrosis. 3. The presence of cardiovascular, cerebrovascular, hepatic, renal, hematopoietic, or other serious primary diseases. 4. Use of medications or supplements containing iron, magnesium, calcium, zinc, or ionic antagonists in the last 30 days. 5. Pregnancy. The stone component composition was determined using a stone infrared spectrum analysis system (Lambda Scientific, Tianjin, China) in the clinical laboratory. Participants in the HC group were from a routine health screening cohort with no history of urinary stones. Samples were collected in the early mornings after fasting and stored at −80 °C until the start of the experiment.

2.2. Metabolite extraction

All samples were randomly labeled, and the sample information was kept blinded throughout the entire experimental process. Each sample was thawed at −80 °C and 100 μL of serum was transferred to a centrifuge tube. Subsequently, 800 μL of precooled methanol/chloroform (1:1) was added, and the mixture was thoroughly vortexed. The metabolite extraction procedure and UPLC–MS experiments were conducted following the protocol described by W. B. Duun et al. [15]. In brief, the mixture was stored at −20 °C and centrifuged at 14,000 rpm for 20 min; this process was repeated three times. Finally, 800 μL of supernatant was collected and dried using nitrogen. A quality control (QC) sample, constructed by pooling serum sample from 5 HCs to 5 RC patients, was included.

2.3. UPLC–MS experiment

Each dried extract was reconstituted in 100 μL of isopropanol/acetonitrile/water (2:1:1) and subjected to UPLC–MS analysis. A Waters SYNAPT G2-Si system equipped with an ACQUITY UPLC-QuanTof mass spectrometer equipped with an ACQUITY UPLC BEH column was used. During the experiment, Leukine Encephalin (LE, m/z 556.2771) and Glu Fibrinopeptide B (GFP, m/z 785.8426) were spiked into the mass spectrometer for mass accuracy monitoring using a dedicated switching probe. A QC sample was analyzed after every 10 samples. The equipment settings are provided in the supplementary materials.

2.4. Data analysis

The raw UPLC-MS data were processed using Progenesis QI 2.0 software and Ezinfo 3.0 (Waters). This included automatic baseline correction, alignment, and peak detection. Peaks that did not meet the 80 % rule were removed. The retained peaks were searched in online libraries such as the Human Metabolome Database (HMDB), Kyoto Encyclopedia of Genes and Genomes (KEGG), ChemSpider, and LipidMAPS for accurate m/z and fragment information. Statistical analysis, including multivariate analysis, Student's t-test, and correlation analysis with clinical data, was performed using SPSS Statistics (ver. 21). Logistic regression analysis was conducted using a forward-wald stepwise variable selection algorithm to retain the most relevant variables for discrimination. Model coefficients, significance, and prediction results of the receiver operating characteristic (ROC) curves were calculated and are provided. Metabolomics pathway analysis (MetPA) was used to identify metabolic pathways enriched for differentially abundant metabolites [16].

3. Results

3.1. Patient characteristics

A total of 45 RC patients (26 with calcium oxalate stones, 12 with calcium phosphate stones, and 7 with uric acid stones) and 48 HC patients were included in this study. The general characteristics of the patients are presented in Table 1.

3.2. Clinical information

This study included a total of 93 serum samples, comprising 45 samples from patients with RC and 48 samples from HC. A summary of the clinical information for the RC patients is presented in Table 2. Significant differences were observed in various serum indicators, including prealbumin (PA), estimated glomerular filtration rate, retinol-binding protein, creatinine, and uric acid, compared to normal ranges. PA, in particular, is synthesized in liver cells and plays a crucial role in transporting thyroxine and vitamin A. Additionally, it possesses thymic hormone activity and promotes lymphocyte maturation, thereby enhancing the body's immune response. The decrease in PA levels among RC patients suggests abnormalities in related metabolism.

3.3. Serum metabolic differences between RC and HC

A total of 93 serum samples were randomly analyzed using electrospray ionization positive and negative ion modes. Partial least squares (PLS) regression analysis revealed significant differences in serum metabolites between the RC and HC groups. The RC group exhibited a greater degree of within-group variation, as evidenced by its looser distribution (Fig. 1A). Subsequently, a more stringent filtering approach was employed to identify differentially abundant metabolites. Signals with VIP >1.0 in orthogonal signal correction (OSC)-PLS loadings were selected, followed by criteria such as a) corrected $P < 0.05$; b) involvement of MS fragmentation patterns in the library search; and c) presence in HMDB and an HMDB library search score >35. Following the removal of exogenous metabolites, a total of 48 compounds with metabolic significance, as documented in the KEGG database, were retained (Supp. Table 1).

Alterations in fatty acids and lipids were observed in the serum metabolites of the two sample groups. Most fatty acids exhibited significantly lower levels in RC sera, including unsaturated fatty acids such as avenoleic acid, 12-oxo-10E-octadecenoic acid, (8E)-10-hydroxy-8-octadecenoic acid, and L-argininium, as well as saturated fatty acids such as 4-oxooctadecanoic acid, hexacosanedioic acid, 16-hydroxy hexadecanoic acid, and 3-oxo-pentadecanoic acid, with the exception of 15S-hydroperoxy-eicosadienoic acid. Moreover, a decreasing trend was observed in RC sera for substances such as linoleamide, epoxy-nonadecadiene, 4-ethylphenylsulfate, and nor-cotinine, which are fatty amides, fatty acyls, ary lsulfates, and pyridine derivatives, respectively. Conversely, the RC group exhibited increased levels of ascorbyl stearate, 3-hydroxy-5, 8-tetradecadienoylcarnitine, and 2-butyl-4-methylphenol.

GPs are characterized by a glycerol molecule with sn-1 and sn-2 esterified by fatty acids and a sn-3 site esterified by phosphoric acid. The OH groups of phosphate are further esterified with choline, ethanolamine, serine, and inositol, generating phosphatidylcholine (PC), phosphatidylethanolamine (PE), phosphatidylserine, and phosphatidylinositol. The substituents at the sn-1 and sn-2 positions result in further diversity. More specifically, a carboxyl bond, an unmodified alkyl ether bond, or an alkenyl ether bond could form at the sn-1 position and are termed diacyl GP, plasmanyl GP, and plasmalogen GP respectively (Fig. 1B). In the present study, multiple PEs varied in RC sera. Among them, all 6 plasmenyl PEs were downregulated, whereas the 8 diacyl PEs were all upregulated in the RC group (Fig. 1C). In addition, the levels of 3 diacyl PCs and plasmanyl phosphatidylglycerols (PGs) were increased in RC sera.

3.4. Correlations between clinical information and metabolic variation

To investigate the underlying association between serum metabolites and RC patients' physiological status, we used Pearson correlation analyses to demonstrate correlations between the 48 differentially abundant metabolites and clinical indicators from patients' blood tests (Fig. 2A and B). Among them, patients' TP was found to be positively correlated with a plasmenyl PE ($P < 0.05$) and negatively correlated with 2 diacyl PEs (PE (16:0/18:1(9Z)), $P < 0.01$; PE (16:0/18:2(9Z,12Z)), $P < 0.05$). Similarly, ALB and PA were negatively correlated with diacyl PEs. On the other hand, Fn and 2 plasmenyl PEs were positively correlated. RBP was negatively correlated with a fatty acid (15S-hydroperoxy-11Z, 13E-eicosadienoic acid, $P < 0.05$) and positively correlated with a fatty acyl (3S,

Table 1
Patient characteristics.

Characteristic	RC group	HC group	*P* value
Number of samples	45	48	–
Age (years)[a]	42 ± 13.2	43.9 ± 14.4	0.7620
Gender (F/M)	17/28	26/22	0.1132
BMI (kg/m^2)[a]	20.9 ± 2.1	22.1 ± 2.2	0.2534
Calcium oxalate (n)	26	–	–
Calcium phosphate (n)	12	–	–
Uric acid (n)	7	–	–

[a] Data are presented as mean ± SD; F: Females; M: Males; BMI: body mass index; n: numbers.

Table 2
Clinical information of the RC patients.

Clinical parameters	Average ± SD	Median ($Q_{25\ \%}$, $Q_{75\ \%}$)	Standard reference interval	Proportion of samples not in the standard range	Variation trend in RC group
Total protein (TP, g/L)	70 ± 5	71 (67, 74)	65–85	18.60 %	↓
PA, mg/L	255 ± 71	254 (226, 290)	250–400	46.51 %	↓
Albumin (ALB, g/L)	45 ± 4	45 (42, 48)	40–55	11.63 %	↓
Fibronectin (Fn, mg/L)	198 ± 28	193 (178, 215)	180–280	27.91 %	↓
β 2-microglobulin (β2-m, mg/L)	2.6 ± 1.1	2.3 (1.9, 3.0)	0.8–2.5	38.46 %	↑
Retinol binding protein (RBP, mg/L)	41 ± 17	40 (30, 50)	36–72	40.48 %	↓
Cystatin C (CYC, mg/L)	1.14 ± 0.42	1.03 (0.90, 1.24)	0–1.16	33.33 %	↑
Creatinine (Cr, μmol/L)	142 ± 157	89 (80, 116)	57–97	48.84 %	↑
Uric acid (UA, μmol/L)	438 ± 100	416 (381, 492)	208–428	44.19 %	↑
Serum sodium (Na, mmol/L)	145 ± 3	144 (142, 147)	137–147	27.91 %	↑
Adjusted Calcium (Ca(adj), mmol/L)	1.90 ± 0.27	1.88 (1.70, 2.04)	2.10–2.37	86.05 %	↓
Estimated glomerular filtration rate (eGFR, mL/min)	75.93 ± 31.86	88.50 (42.94, 94.01)	>90	56.41 %	↓

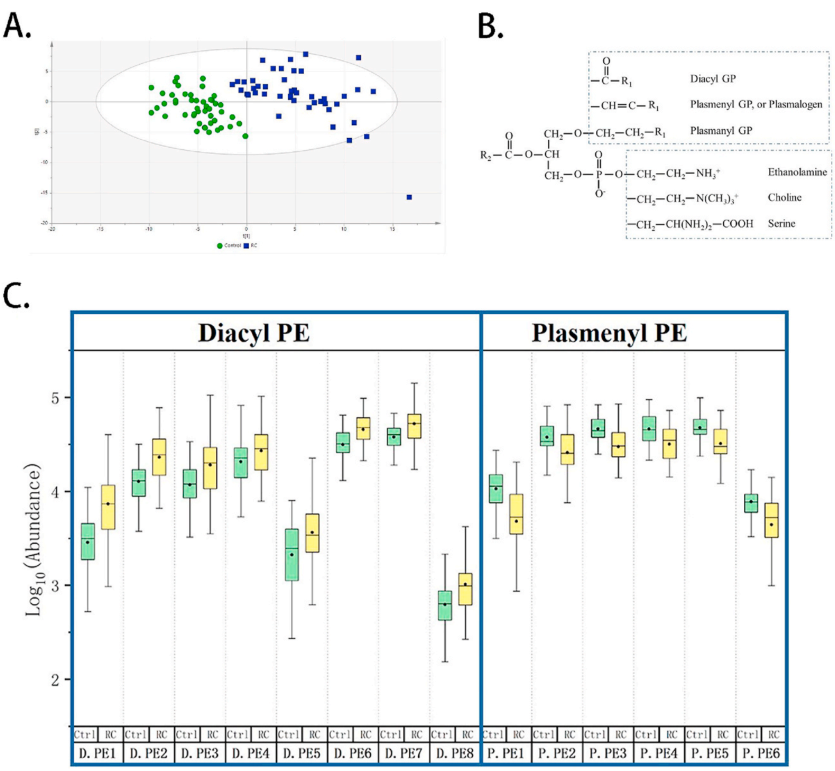

Fig. 1. (A) PLS score plot illustrating separate clustering of serum samples by group. (B) Structure of GP. (C) The abundances with log10 transformation of diacy PEs (D. PEs) and plasmenyl Pes (P. PEs) are presented in a box plot. D.PE1 = PE(16:0/18:1(9Z)), D.PE2 = PE(16:0/18:2(9Z,12Z)), D.PE3 = PE(16:0/20:4(8Z,11Z,14Z,17Z)), D.PE4 = PE(16:0/22:6(4Z,7Z,10Z,13Z,16Z,19Z)), D.PE5 = PE(18:0/18:1(9Z)), D.PE6 = PE(18:0/18:2(9Z,12Z)), D.PE7 = PE(18:0/20:4(5Z,8Z,11Z,14Z)), D.PE8 = PE(18:1(11Z)/22:4(7Z,10Z,13Z,16Z)). P.PE1 = PE(18:2(9Z,12Z)/P-18:0), P.PE2 = PE(20:4(5Z,8Z,11Z,14Z)/P-16:0), P.PE3 = PE(20:4(5Z,8Z,11Z,14Z)/P-18:1(11Z)), P.PE4 = PE(P-18:0/20:4(5Z,8Z,11Z,14Z)), P.PE5 = PE(P-16:0/22:6(4Z,7Z,10Z,13Z,16Z,19Z)), P.PE6 = PE(16:1(9Z)/P-18:1(11Z)). RC refers to the RC group, Ctrl refers to the HC group.

4R-epoxy-6Z,9Z-nonadecadiene, $P < 0.05$). In terms of the common monitoring indices of RC, uric acid was positively correlated with both diacyl PE and diacyl PC. Positive correlations were also observed between the eGFR and plasmenyl PE, as well as between the eGFR and the levels of fatty amides. Calcium levels appeared to have a negative correlation with diacyl PC.

3.5. Metabolic biomarker model for RC diagnosis

Logistic regression with the forward wald variable selection algorithm was utilized to construct the RC diagnostic model using serum metabolic biomarkers. In the regression, RC patients were labeled “1″, and healthy controls were labeled “0″ for the dependent

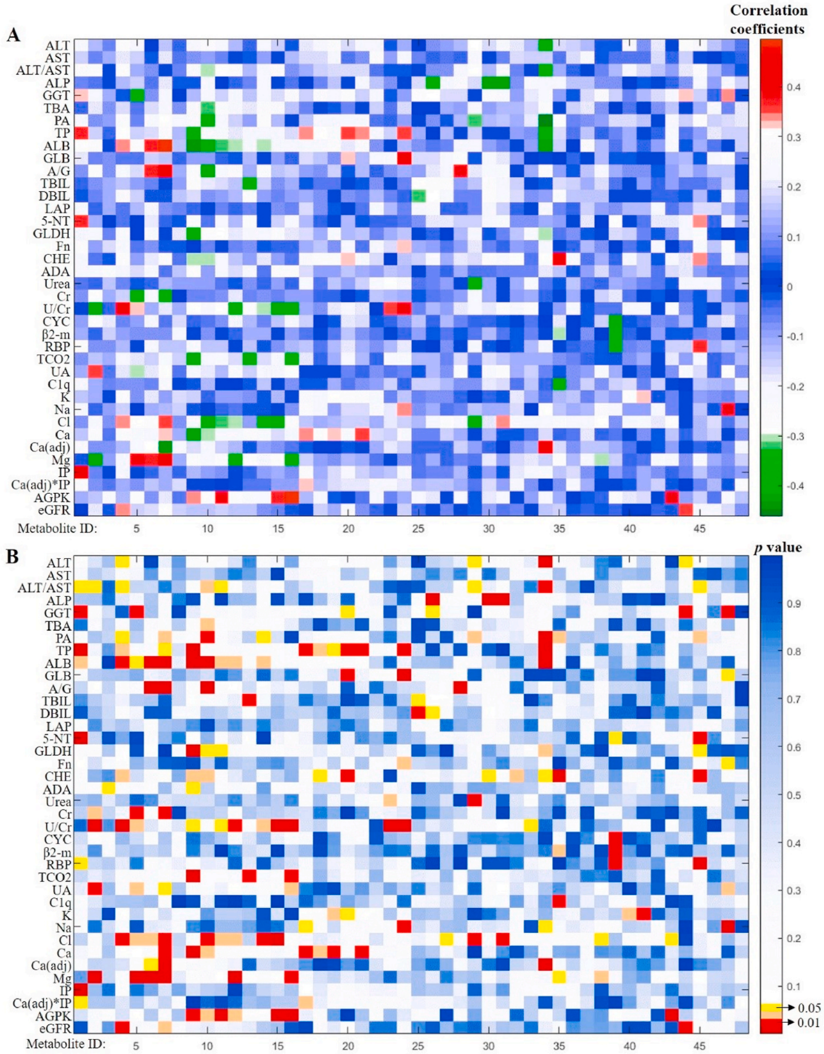

Fig. 2. Maps of Spearman correlation coefficients between metabolites detected by UPLC–MS and clinical parameters. (A) Pairwise correlation coefficients; (B) pairwise correlation significance of *P* values. The y-axis shows the corresponding clinical information, and the x-axis shows the metabolite ID detected by mass spectrometry.

variable. All 48 metabolites were included in the model, which automatically retained the most discriminant variables, including 2 plasmenyl PEs, 2 fatty acids, 1 fatty amide, 1 arylsulfate, and 1 cresol (Table 3). The overall prediction accuracy was 94.6 %, with an area under the ROC curve (AUROC) of 1.00 (concordance index (CI): 0.99~1.00), indicating a favorable discriminative capability. From the model coefficients, it was observed that a higher level of 2-butyl-4-methyl phenol (cresols) and a lower level of PE (P-16:0/22:6(4Z,7Z,10Z,13Z,16Z,19Z)), a plasmenyl PE, contributed the most to the risk of RC occurrence.

3.6. Metabolic pathway disturbance in RC patients

To identify the disturbed metabolic pathways in RC patients, the 48 identified compounds were first input into MetPA, an online tool that facilitates integrative analysis of metabolomics data. The pathway analysis results are presented in Fig. 3A, where the y-axis represents the -log (*P* values) of the involved pathway enrichment analysis, and the x-axis represents the corresponding pathway impact value of topology analysis. A total of 5 metabolic pathways were identified, 4 of which were significantly different ($P < 0.05$) (Table 4). These pathways include GP metabolism, linoleic acid metabolism, α-linolenic acid metabolism, and glycosylphosphatidylinositol (GPI)-anchor biosynthesis. The last three metabolic pathways were highlighted by PC, which also is involved in GP metabolism. By referencing the literature and KEGG, a more comprehensive pathway map (Fig. 3B) was created, illustrating the metabolites with significant differences in RC sera, with a focus on plasmenyl PEs. The entire map mainly encompasses GP metabolism, glycerolipid metabolism, ether lipid metabolism, and sphingophospholipid metabolism.

Table 3
Logistic regression (Forward-Wald) model for RC diagnosis using metabolic biomarkers.

Metabolite ID	Putative identification	Coefficient details			Model parameter					
		B	Wald	Sig.	Cox & Snell R Square	Nagelkerke R Square	Overall predicted percentage	ROC Area	95 % CI Lower Bound	95 % CI Upper Bound
Met.17	PE(18:2(9Z,12Z)/P-18:0)	−5.13	3.19	7.40E-02	0.70	0.94	94.6	1.00	0.99	1.00
Met.20	PE(P-16:0/22:6 (4Z,7Z,10Z,13Z,16Z,19Z))	−8.28	3.92	4.80E-02						
Met.30	Avenoleic acid	−3.55	4.49	3.40E-02						
Met.34	16-Hydroxy hexadecanoic acid	−6.43	4.50	3.40E-02						
Met.44	Linoleamide	−5.89	4.88	2.70E-02						
Met.46	4-Ethylphenylsulfate	−3.87	2.30	1.30E-01						
Met.47	2-Butyl-4-methylphenol	16.63	4.54	3.30E-02						

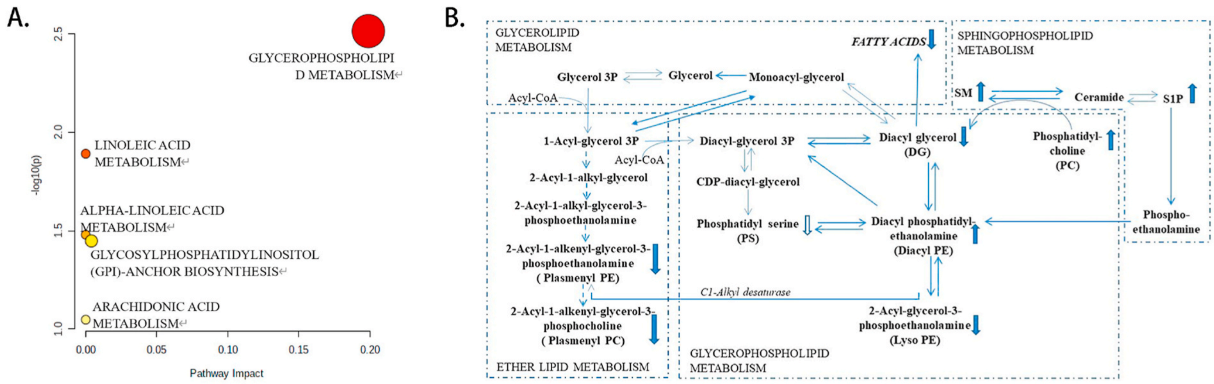

Fig. 3. (A) Altered metabolisms in RC sera suggested by MetPA, including GP metabolism, linoleic acid metabolism, alpha-linoleic acid metabolism, GPI-anchor biosynthesis, and arachidonic acid metabolism. (B) Metabolic pathway diagram showing altered metabolites in RC sera. Upward (downward) arrows indicate significantly higher (lower) levels ($P < 0.05$) in RC.

Table 4
Results of the MetPA of 48 differential serum metabolites from RC patients.

Metabolic Pathway	Total	Expected	Raw p	-LOG10(p)	Holm adjust	FDR	Impact
GP metabolism	36	9.3E-02	3.1E-03	2.51	0.26	0.26	0.20
Linoleic acid metabolism	5	1.3E-02	1.3E-02	1.89	1.00	0.54	0.00
alpha-Linolenic acid metabolism	13	3.4E-02	3.3E-02	1.48	1.00	0.75	0.00
GPI-anchor biosynthesis	14	3.6E-02	3.6E-02	1.45	1.00	0.75	0.00
Arachidonic acid metabolism	36	9.3E-02	9.0E-02	1.05	1.00	1.00	0.00

4. Discussion

In the present study, we are the first to comprehensively investigate the serum metabolite profile of patients with RC using UPLC−MS. We observed diverse metabolic signatures in the sera of RC patients. Furthermore, we identified 48 fluctuating metabolites, primarily fatty acids, fatty acyls, and lipids, with a significant disturbance in the GP-related metabolic pathway, which is associated with disease status.

GP plays a crucial role in regulating transport, signal transduction, and protein function as the main structural lipid in mammalian cell membranes. Diacyl PC, a key metabolite in GP metabolism, serves as a starting substance in the metabolism of linoleic acid and α-linolenic acid. The increased abundance of diacyl PC in the RC group suggested abnormalities in both of these metabolic pathways. Seventy percent of PC is synthesized via CDP choline metabolism, where the conversion of phosphocholine to CDP choline is catalyzed by the rate-limiting enzyme CTP: cytidylinosyltransferase [17,18]. The remaining PC is derived from the PE N-methyltransferase (PEMT) pathway, in which PEMT catalyzes the methylation of PE to form PC. The PEMT pathway ensures sufficient levels of PC and choline for energy metabolism while maintaining the balance of the PC:PE ratio in the body [18,19]. PC can interact with fats, cholesterol, and proteins to form lipid-protein complexes [20]. Lipoproteins, which can easily dissolve in plasma, serve as a mode of fat transport. It has been reported that high triglyceride levels can increase oxalate and uric acid concentrations in urine and decrease urine pH, which are important factors contributing to the occurrence of RC [21]. Our data indicate a positive correlation between increased diacyl PC abundance and uric acid levels, as well as a negative correlation with calcium content. This strongly suggests that abnormally high levels of PC may be one of the direct causes of RC.

In addition, GP metabolism indirectly influences GPI-anchor biosynthesis through the intermediate metabolite diacyl PE. Diacyl PEs can upregulate GPI-anchor biosynthesis, which in turn affects the content of GPI anchor proteins, activating antigens in the immune system. Modified by major histocompatibility complex molecules, GPI anchor proteins contribute to the anti-inflammatory response of macrophages, cell activation, complement cascade amplification, cell proliferation, leukocyte extravasation, tumor invasion, and metastasis [22].

The level of diacyl PE can increase from both upstream and downstream sources, either due to decreased consumption of diacyl PE or increased production of PE. The upregulated sphingophospholipid metabolism may contribute to the increased production of diacyl PE through phosphoethanolamine. Additionally, the balance of diacyl PEs and diacyl PCs is maintained through PEMT, as mentioned previously. Another possible cause of increased diacyl PE is the abnormal conversion of diacyl PE to plasmenyl PE, which is supported by evidence of decreased plasmenyl PE levels.

In our study, we found that plasmenyl PE and plasmenyl PC were significantly less abundant in the sera of RC patients than in those of healthy individuals. Both of these lipids belong to the plasmalogen family, which has distinct functions due to the presence of vinyl ether bonds at the sn-1 position. These bonds align the sn-1 and sn-2 chains parallel to each other, reducing the fluidity of the aliphatic chain and facilitating the formation of the non-bilayers necessary for fusion and fission processes. Moreover, plasmalogens are more susceptible to free radicals and oxygen than diacyl GP due to their structure [23]. Plasmalogens are sacrificial in nature, protecting polyunsaturated fatty acids and other delicate membrane lipids from oxidation [24]. Furthermore, they serve as reservoirs for DHA biosynthesis, and their derivatives play a role in regulating inflammation [25]. Plasmalogen deficiency also impairs the cholesterol pool required for efflux [26,27]. In this study, the abnormally low abundance of plasmenyl PEs in RC patients may be attributed to the high level of reactive oxygen species, leading to excessive consumption of plasmenyl PEs in the antioxidant response. Additionally, the decreased plasmenyl PE levels could be a result of insufficient formation, which includes 1) abnormalities in the transformation from diacyl PE to plasmenyl PE by C1-alkyl desaturase and 2) deficiencies in DG and downregulated GP metabolism, resulting in insufficient synthesis of plasmenyl PEs through glycerol GPs. It would be worthwhile to explore the enzymes involved in GP metabolism and ether lipid metabolism in future research. Furthermore, in RC patients, we observed a positive correlation between reduced protein levels and plasmenyl PEs. This reduction in plasmalogen levels and its adverse impact on cholesterol efflux have also been observed in patients with end-stage renal disease, compared to those with mild-to-moderate chronic kidney disease [26].

Based on the identification of differential metabolic biomarkers in patients with RC, we developed a classical logistic regression model for RC diagnosis. Through the use of a variable selection algorithm, the final model retained only seven metabolic biomarkers but demonstrated excellent discriminative ability. It is important to note that two of the seven markers were plasmanyl PE, whereas the other two were closely related to fatty acids, highlighting the significant disturbance of GP metabolism in RC patients. Although further analysis and optimization are needed, our results indicate the potential of using serum biomarkers for RC diagnosis. We are currently expanding our sample set for more robust analysis and plan to conduct in vitro validation experiments to establish the associations between serum biomarkers and urine chemical composition.

Currently, the clinical diagnosis of RC relies on imaging techniques such as ultrasound, radiographs, and computed tomography. However, these methods can only discriminate the presence or absence of stones and cannot identify renal crystal deposits in patients who have not yet formed stones or who have had stones removed surgically. Metabolite-based diagnostic models have the potential to predict stone development and provide guidance for stone prevention in these patients. Furthermore, the disorganized metabolic pathways and molecules identified in this study offer potential targets for understanding the pathological mechanisms of RC formation. However, it is important to acknowledge the limitations of this study, such as the insufficient sample size given the high prevalence of RC. To address this, we are expanding our sample set for further analysis. Additionally, the use of UPLC−MS for detection is associated with procedural complexity, long detection times, and limited detection range. Clinical validation will provide strong evidence to support our diagnostic model, and we plan to incorporate this in future studies.

5. Conclusion

The present study yielded two notable findings. First, it should be noted that this study is pioneering in its investigation of metabolic alterations in RC serum using UPLC−MS. The differentially abundant metabolites identified in this study indicate that the primary perturbation manifests around GP metabolism. There is suggestive evidence to support the notion that upregulated diacyl PC may directly trigger elevated uric acid levels and reduced calcium levels. Additionally, a series of abnormally low levels of plasmenyl PEs offer valuable insights for understanding the pathology of RC. Second, the discriminative model developed in this study provides concrete evidence of a viable approach for diagnosing RC using serum metabolites in the future. These findings significantly enhance our understanding of RC physiology from a metabolomics perspective. Moving forward, future research should consider examining the related chemical composition of urine, conducting protein and gene analysis, exploring variations and optimizing the diagnostic model using new sample cohorts.

Data availability

All data will be made available on request.

CRediT authorship contribution statement

Yunhe Xiong: Writing – original draft, Validation, Project administration, Methodology, Investigation. **Qianlin Song:** Visualization, Validation, Investigation, Formal analysis, Data curation. **Shurui Zhao:** Software, Resources, Investigation. **Chuan Wang:** Supervision, Project administration. **Hu Ke:** Validation, Investigation, Formal analysis. **Wenbiao Liao:** Supervision, Resources. **Lingchao Meng:** Resources, Methodology. **Lingyan Liu:** Writing – review & editing, Funding acquisition, Conceptualization. **Chao Song:** Writing – review & editing, Writing – original draft, Visualization, Conceptualization.

Declaration of competing interest

The authors declare that they have no known competing financial interests or personal relationships that could have appeared to influence the work reported in this paper.

Acknowledgements

This work was financially supported by the National Natural Science Foundation of China (No. 81901554).

Appendix A. Supplementary data

Supplementary data to this article can be found online at https://doi.org/10.1016/j.heliyon.2024.e32482.

References

[1] S.R. Khan, M.S. Pearle, W.G. Robertson, G. Gambaro, B.K. Canales, S. Doizi, O. Traxer, H.G. Tiselius, Kidney stones, Nat. Rev. Dis. Prim. 2 (2016) 16008.
[2] R. Palsson, O.S. Indridason, V.O. Edvardsson, A. Oddsson, Genetics of common complex kidney stone disease: insights from genome-wide association studies, Urolithiasis 47 (2019) 11–21.
[3] F.R. Spivacow, E.E. Del Valle, E. Lores, P.G. Rey, Kidney stones: composition, frequency and relation to metabolic diagnosis, Medicina (B Aires) 76 (2016) 343–348.
[4] R. Siener, Nutrition and kidney stone disease, Nutrients 13 (2021).
[5] W. Wang, J. Fan, G. Huang, J. Li, X. Zhu, Y. Tian, L. Su, Prevalence of kidney stones in mainland China: a systematic review, Sci. Rep. 7 (2017) 41630.
[6] S. Nackeeran, J. Katz, R. Ramasamy, R. Marcovich, Association between sex hormones and kidney stones: analysis of the national health and nutrition examination survey, World J. Urol. 39 (2021) 1269–1275.
[7] Z. Ye, G. Zeng, H. Yang, J. Li, K. Tang, G. Wang, S. Wang, Y. Yu, Y. Wang, T. Zhang, Y. Long, W. Li, C. Wang, W. Wang, S. Gao, Y. Shan, X. Huang, Z. Bai, X. Lin, Y. Cheng, Q. Wang, Z. Xu, L. Xie, J. Yuan, S. Ren, Y. Fan, T. Pan, J. Wang, X. Li, X. Chen, X. Gu, Z. Sun, K. Xiao, J. Jia, Q. Zhang, G. Wang, T. Sun, X. Li, C. Xu, C. Xu, G. Shi, J. He, L. Song, G. Sun, D. Wang, Y. Liu, C. Wang, Y. Han, P. Liang, Z. Wang, W. He, Z. Chen, J. Xing, H. Xu, The status and characteristics of urinary stone composition in China, BJU Int. 125 (2020) 801–809.
[8] C. Boonla, P. Tosukhowong, B. Spittau, A. Schlosser, C. Pimratana, K. Krieglstein, Inflammatory and fibrotic proteins proteomically identified as key protein constituents in urine and stone matrix of patients with kidney calculi, Clin. Chim. Acta 429 (2014) 81–89.
[9] C. Thongprayoon, I. Vuckovic, L.E. Vaughan, S. Macura, N.B. Larson, M.R. D'Costa, J.C. Lieske, A.D. Rule, A. Denic, Nuclear magnetic resonance metabolomic profiling and urine chemistries in incident kidney stone formers compared with controls, J. Am. Soc. Nephrol. 33 (2022) 2071–2086.
[10] A. Primiano, S. Persichilli, P.M. Ferraro, R. Calvani, A. Biancolillo, F. Marini, A. Picca, E. Marzetti, A. Urbani, J. Gervasoni, A specific urinary amino acid profile characterizes people with kidney stones, Dis. Markers 2020 (2020) 8848225.
[11] X.Z. Zhang, X.X. Lei, Y.L. Jiang, L.M. Zhao, C.Y. Zou, Y.J. Bai, Y.X. Li, R. Wang, Q.J. Li, Q.Z. Chen, M.H. Fan, Y.T. Song, W.Q. Zhang, Y. Zhang, J. Li-Ling, H. Q. Xie, Application of metabolomics in urolithiasis: the discovery and usage of succinate, Signal Transduct. Targeted Ther. 8 (2023) 41.
[12] Y. Chao, N. Li, S. Xiong, G. Zhang, S. Gao, X. Dong, Lipidomics based on liquid chromatography-high resolution mass spectrometry reveals the protective role of peroxisome proliferator-activated receptor alpha on kidney stone formation in mice treated with glyoxylate, J. Separ. Sci. 46 (2023) e2300452.
[13] Z. Zhou, D. Feng, D. Shi, P. Gao, L. Wang, Z. Wu, Untargeted and targeted metabolomics reveal bile acid profile changes in rats with ethylene glycol-induced calcium oxalate nephrolithiasis, Chem. Biol. Interact. 381 (2023) 110570.
[14] J. Wen, Y. Cao, Y. Li, F. Zhu, M. Yuan, J. Xu, J. Li, Metabolomics analysis of the serum from children with urolithiasis using UPLC-MS, Clin Transl Sci 14 (2021) 1327–1337.
[15] W.B. Dunn, D. Broadhurst, P. Begley, E. Zelena, S. Francis-McIntyre, N. Anderson, M. Brown, J.D. Knowles, A. Halsall, J.N. Haselden, A.W. Nicholls, I.D. Wilson, D.B. Kell, R. Goodacre, C. Human Serum Metabolome, Procedures for large-scale metabolic profiling of serum and plasma using gas chromatography and liquid chromatography coupled to mass spectrometry, Nat. Protoc. 6 (2011) 1060–1083.
[16] J. Xia, D.S. Wishart, MetPA: a web-based metabolomics tool for pathway analysis and visualization, Bioinformatics 26 (2010) 2342–2344.
[17] C.R. McMaster, R.M. Bell, CDP-choline:1,2-diacylglycerol cholinephosphotransferase, Biochim. Biophys. Acta 1348 (1997) 100–110.
[18] J.N. van der Veen, J.P. Kennelly, S. Wan, J.E. Vance, D.E. Vance, R.L. Jacobs, The critical role of phosphatidylcholine and phosphatidylethanolamine metabolism in health and disease, Biochim. Biophys. Acta Biomembr. 1859 (2017) 1558–1572.
[19] R.K. Mallampalli, A.J. Ryan, R.G. Salome, S. Jackowski, Tumor necrosis factor-alpha inhibits expression of CTP:phosphocholine cytidylyltransferase, J. Biol. Chem. 275 (2000) 9699–9708.
[20] J.N. van der Veen, J.P. Kennelly, S. Wan, J.E. Vance, D.E. Vance, R.L. Jacobs, The critical role of phosphatidylcholine and phosphatidylethanolamine metabolism in health and disease, Biochim. Biophys. Acta Biomembr. 1859 (2017) 1558–1572.
[21] F.C. Torricelli, S.K. De, S. Gebreselassie, I. Li, C. Sarkissian, M. Monga, Dyslipidemia and kidney stone risk, J. Urol. 191 (2014) 667–672.

[22] P.M. Krawitz, Y. Murakami, J. Hecht, U. Kruger, S.E. Holder, G.R. Mortier, B. Delle Chiaie, E. De Baere, M.D. Thompson, T. Roscioli, S. Kielbasa, T. Kinoshita, S. Mundlos, P.N. Robinson, D. Horn, Mutations in PIGO, a member of the GPI-anchor-synthesis pathway, cause hyperphosphatasia with mental retardation, Am. J. Hum. Genet. 91 (2012) 146–151.
[23] A. Broniec, R. Klosinski, A. Pawlak, M. Wrona-Krol, D. Thompson, T. Sarna, Interactions of plasmalogens and their diacyl analogs with singlet oxygen in selected model systems, Free Radic. Biol. Med. 50 (2011) 892–898.
[24] P.J. Sindelar, Z. Guan, G. Dallner, L. Ernster, The protective role of plasmalogens in iron-induced lipid peroxidation, Free Radic. Biol. Med. 26 (1999) 318–324.
[25] M.J. Stables, D.W. Gilroy, Old and new generation lipid mediators in acute inflammation and resolution, Prog. Lipid Res. 50 (2011) 35–51.
[26] R. Maeba, K.I. Kojima, M. Nagura, A. Komori, M. Nishimukai, T. Okazaki, S. Uchida, Association of cholesterol efflux capacity with plasmalogen levels of high-density lipoprotein: a cross-sectional study in chronic kidney disease patients, Atherosclerosis 270 (2018) 102–109.
[27] N.E. Braverman, A.B. Moser, Functions of plasmalogen lipids in health and disease, Biochim. Biophys. Acta 1822 (2012) 1442–1452.